Ad van der Spek

C-9657 716

Studyreport W.W.K. 70 - 16

LITTORAL DRIFT IN THE SURF ZONE

by

Ir. W. T. Bakker

CONTENTS

LITTORAL DRIFT IN THE SURF ZONE

Lecture, held at the Hydraulic Research Station, Wallingford on December 15, 1970 [1]

0. INTRODUCTION

I should like to talk about the question of what happens to a coast after the building of constructions such as groynes or harbour moles.

So first, (in chapter 1) we shall consider the forces acting on the grains in the surf zone, then (in chapter 2) some transport formulae, used in the Netherlands and finally (chapter 3) mathematical models of coasts with groynes or harbour moles.

1. FORCES IN THE BREAKER ZONE

1.1 Shear stress over the bottom

Most probable the waves stir up the sand grains and the currents transport them. So it is worth while to estimate the shear stress of the water over the bottom, which causes the stirring up.

The waves give an orbital velocity u (changing constantly) and a longshore velocity v (remaining almost stationary). In the breaker zone the waves are nearly perpendicular to the coast, and thus the resultant velocity will be about $\sqrt{u^2 + v^2}$ at every moment (fig. 1[a])

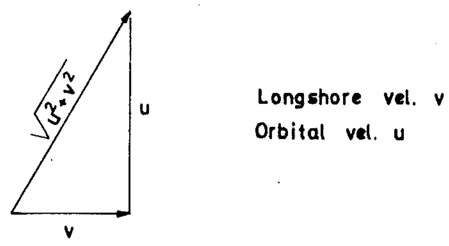

Fig. 1[a] Water velocities

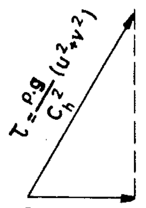

$$\tau_{longshore} = \frac{v}{\sqrt{u^2+v^2}} \cdot \frac{\rho . g}{C_h^2} \cdot (u^2+v^2) = \frac{\rho . g}{C_h^2} . v \sqrt{u^2+v^2}$$

Fig. 1[b] Bottom shear stress

---

1) revised, April 1971

The shear stress τ has of course the same direction as the instantaneous velocity and has the magnitude (fig. 1[b]):

$$\tau = \frac{\rho g}{C_h^2} (u^2 + v^2),$$

proportional to the square of the water velocity and to the specific weight ρg, C_h being the Chezy-coefficient.

The longshore component $\tau_{\mathbf{longshore}}$ of this velocity is (fig. 1[b]):

$$\tau_{\mathbf{longshore}} = \frac{\rho g}{C_h^2} v \sqrt{u^2 + v^2} \qquad \ldots\ldots\ldots\ldots (1^a)$$

However, this reasoning is a little over-simplified as it is assumed that the combined velocity $\sqrt{u^2 + v^2}$ has a logarithmic distribution over the vertical.

Probably the BIJKER-approach [1] is better; he considers the shear stress on the boundary layer and finds instead of (1^a) ([1], formula III.3.14 with $\varphi = 0^\circ$):

$$\tau_{\text{longshore}} = \rho v_*^2 \sqrt{\frac{p^2 K^2 C_h^2}{g} \frac{u^2}{v^2} + 1}$$

in which p is a constant ($\simeq 0.42$), K is the constant of **VON** KARMAN ($\simeq 0.4$) and v_* is the boundary shear stress:

$$v_* = v \sqrt{g/C_h^2}$$

This can be reduced to a shape similar to (1^a):

$$\tau_{\mathbf{longshore}} = \frac{\rho g}{C_h^2} v \sqrt{\left(\frac{pKC_h}{\sqrt{g}} u\right)^2 + v^2} \qquad \ldots\ldots\ldots\ldots (1^b)$$

to compare with (1^a):

$$\tau_{\mathbf{longshore}} = \frac{\rho g}{C_h^2} v \sqrt{u^2 + v^2} \qquad \ldots\ldots\ldots\ldots (1^a)$$

However, it remains a curious fact, that the BIJKER-solution [1] does not tend to (1^a) for long-period waves; this justifies future research in this field.

In the meantime we shall assume that (1^b) is valid.

Averaged over a wave period τ **longshore** **amounts to:**

$$\overline{\tau}_{\text{longshore}} = \frac{\rho g}{C_h^{\;2}}\, v \sqrt{(pKC_h u/\sqrt{g})^2 + v^2} \quad \ldots\ldots\ldots\ldots \quad (2)$$

The value of the term "$pKC_h/\sqrt{g}$" **usually equals approximately** 2 to 3 and hence the term "$(pKC_h\hat{u}/\sqrt{g})^2$" **is usually large with** respect to v^2 in the surf zone.

Fig. 2 shows the factor $\sqrt{(pKC_h u/\sqrt{g})^2 + v^2}$ **in the case** $pKC_h\hat{u}/\sqrt{g} = 5v$.

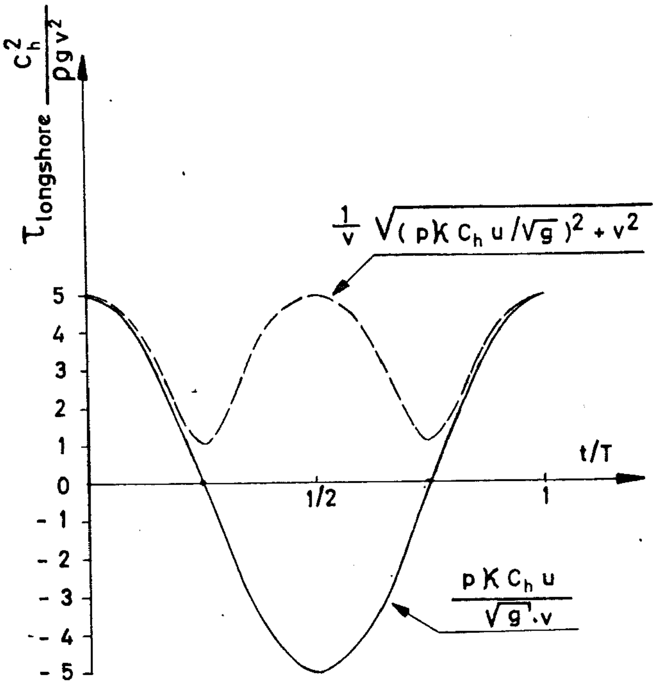

Fig. 2 $\tau_{\text{longshore}}$ and orbital velocity as function of t/T

When v is small with respect to u, $\overline{\tau}$ **longshore** becomes approximately

$$\tau_{\text{longshore}} = \frac{2}{\pi}\, pK\sqrt{f/8}\,.\,\rho\,\hat{u}v \quad \ldots\ldots\ldots\ldots \quad (3)$$

The factor $8\ g/C_h^2$ has been replaced by the DARCY-WEISBACH friction coefficient f in (3).

In his paper on longshore currents, BOWEN [2] linearises the relation between τ_{bottom} and v:

$$\tau_{bottom} = c_f v \quad \text{(4)}$$

(c_f equals "ρ c" in BOWEN's notation).

From (3) we find, that the factor c_f is proportional to $\hat{u}$:

$$c_f = \frac{2}{\pi} \cdot pK \sqrt{f/8} \cdot \rho \hat{u} \quad \text{(5)}$$

$\hat{u}$ in the breaker zone equals (linear theory):

$$\hat{u} = \frac{H}{2} \sqrt{g/D} \quad (6^a)$$

Taking the ratio between H and D in the case of a spilling breaker equal to A_2, we find:

$$\hat{u} = \frac{A_2}{2} \sqrt{gD} \quad (6^b)$$

In the case of a wave spectrum, it might be questionable as to which $\hat{u}$ should be taken.
In order to get the mean longshore velocity, it seems reasonable, since c_f is proportional to $\hat{u}$, to take the $\hat{u}$, corresponding to the mean wave height.

We define:

$$A_2 = \overline{H}/D \text{ in the breaker zone} \quad \text{(7)}$$

One finds for c_f; from (5) and (6^b):

$$c_f = \frac{1}{\pi\sqrt{8}} pK\ A_2 \rho \sqrt{fgD} \quad \text{(8)}$$

In many papers [4], [5], [6] about longshore velocity the shear stress is taken proportional to v^2. It appears to be much larger than this however.

BIJKER [1] , [7] computed the longshore component of the shear stress more accurately than by the rough approximation given here.

He computed $\overline{\tau}_{longshore} / \tau_o$ as a function of $\frac{p K C_h}{\sqrt{g}} \frac{\hat{u}}{v}$, in which τ_o is the shear stress without waves:

$$\tau_o = \frac{\rho g}{C_h^{\,2}} \; v^2$$

From (2) can be derived:

$$\frac{\overline{\tau}_{\mathbf{longshore}}}{\tau_o} = \sqrt{\left(\frac{p K C_h}{\sqrt{g}} \; \frac{u}{v}\right)^2 + 1} \qquad \ldots\ldots\ldots\ldots\ldots\ldots \; (2^b)$$

This function, computed by BIJKER is shown in annex 1 **(solid line).**
As an interrupted line is shown the approximation according to (3):

$$\frac{\overline{\tau}_{longshore}}{\tau_o} = \frac{2}{\pi} \; \frac{p K C_h}{\sqrt{g}} \; \frac{\hat{u}}{v} \qquad \ldots\ldots\ldots\ldots\ldots\ldots \; (3^b)$$

It is curious, that BIJKER uses in [7] the EAGLESON computation for the longshore velocity, which is based on proportionality of τ with v^2.

1.2 Radiation stress

We have considered the friction; now we shall consider the driving force in the breaker zone.

The driving force of the wave is the longshore component of the "radiation stress" [8] , [9] . This radiation stress can be visualized in the set-up of waves on a sloping beach. It consists of two components:

1^o the average pressure $\overline{p}$ over a wave period differs (in second order) from the hydrostatic pressure. This first component is thus an isotropic pressure.

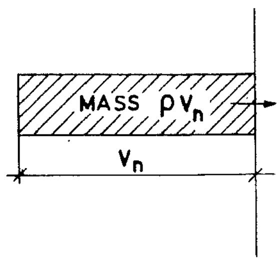

Fig. 3

2^o flux of momentum can be considered as a force; through any cross-section per unit of time and per unit of area a flux $\rho v_n . v$ is transported, if v_n is the component of the velocity perpendicular to the area.
The average over a wave period is not equal to zero. Therefore this second component of the radiation stress is an unidirectional force.

Combined, the first and the second component give a stress field with different principal stresses. It can be visually demonstrated in a Mohr circle (fig. 4).

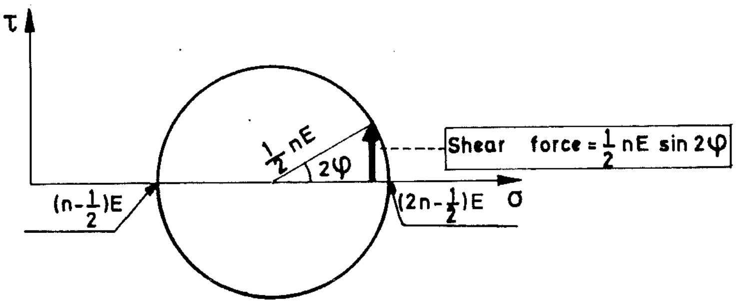

Fig. 4 Mohr circle, representing the radiation stress.

Now the "radiation stress" is by definition this stress field, but integrated over the depth:

$$\text{radiation stress} = \overline{\int_{-D}^{\eta} (p + \rho v_n^2)\, dz} \qquad \text{.......... (9)}$$

in which z is the vertical component with respect to the still-water level and η is the water level.
In fact, the "radiation stress" is not a stress, but a force per unit of length. The dimension is $[mt^{-2}]$.

LONGUET-HIGGINS and STEWART [8] **computed the first and second** component (fig. 4):

$$\left.\begin{array}{l} \overline{\int_{-D}^{\eta} (p - p_o)\, dz} = (n - \tfrac{1}{2})\, E \quad \text{(isotropie)} \\ \\ \text{and} \quad \int_{-D}^{\eta} \rho u^2\, dz = n\, E \quad \text{(in the direction of u)} \end{array}\right\} \text{............. (10)}$$

in which E is the wave energy per unit of area and n is the ratio between phase and group velocity.
So the principal stress in the direction of wave propagation is $(n - \frac{1}{2} + n)$ E; in the direction of the wave crest on the other hand, where the momentum ρu^2 gives no component, it is $(n - \frac{1}{2})$ E.
Thus (fig. 4), the radius of the Mohr circle, representing this stress field is $\frac{1}{2}$ nE and therefore, in a vertical plane, making an angle φ with the wave crest, the shear force F_{wave} is $\frac{1}{2}$ nE sin 2φ.

The force, perpendicular to this plane, $(1\frac{1}{2}n - \frac{1}{2})E + \frac{1}{2}$ nE cos 2φ, causes set-up, and the above mentioned shear force a longshore velocity.

1.3 Tidal force compared with radiation stress [10]

We consider the water mass above a rigid slope z = my up to the breaker line (fig. 5).
On this mass the shear force mentioned in 1.2 acts in the plane ABCD.
Calling this shear force F_{wave}, this force equals:

$$F_{wave} = \tfrac{1}{2}\, nE \sin 2\varphi \quad \ldots\ldots (11)$$

In the breaker zone may be stated:

$$n = 1 \quad \ldots\ldots\ldots\ldots (12)$$

$$E = \frac{1}{8}\rho g\, \bar{H}_{br}^{\,2} \quad \ldots\ldots (13)$$

$$\bar{H}_{br} = A_2\, D_{br} \quad \ldots\ldots (14)$$

Thus for the wave force is found:

$$F_{wave} = \frac{1}{16}\rho g\, A_2^{\,2} D_{br}^{\,2} \sin 2\varphi \quad \ldots\ldots (15)$$

The tidal force on this triangular prism of water equals:

$$F_{tide} = \rho g\, \frac{\partial h}{\partial x} \cdot (\text{area}) = \rho g\, \frac{\partial h}{\partial x} \cdot \frac{1}{2m} D_{br}^{2} \quad \ldots (16)$$

in which h is the elevation of the water level and x the longshore direction.

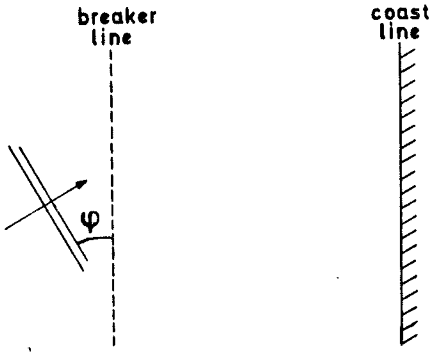

Fig. 5^a
Plan view.

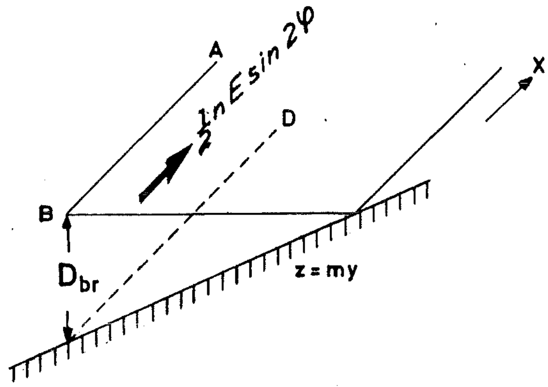

Fig. 5^b

Consider a progressive tidal wave with amplitude $\hat{z}$:

$$h = \hat{z} \cos(\omega t - Kx) \quad \ldots\ldots\ldots\ldots\ldots\ldots\ldots\ldots\ldots\ldots (17)$$

In this case the ratio of wave force to tidal force equals:

$$\frac{F_{wave}}{F_{tide}} = \frac{A_2^{\,2}\, m \sin 2\varphi_{br}}{8\, K\, \hat{z}} \quad \ldots\ldots\ldots\ldots\ldots\ldots\ldots\ldots\ldots\ldots (18)$$

Measurements of SVAŠEK [11] and KOELÉ/de BRUYN [12] showed, that in the breaker zone the ratio between H_{sign} and D in the prototype, for gentle sloping beaches is about .4 to .5.
Thus the ratio between $\bar{H}$ and D will be about .3 to .4.
Theoretically, for a solitary wave on a flat bottom, the ratio is .78 and in the laboratory, on slopes of about 1 : 8 or 1 : 10 values up to 1.1 are measured.

From (17) it can be seen, that often the wave force is large with respect to the tidal force in the breaker zone. This may be illustrated with the following example:

$$\frac{F_{wave}}{F_{tide}} = 20 \sin 2\varphi_{br} \text{ if } \begin{array}{l} m = 10^{-2} \\ A_2 = .4 \end{array} \quad \begin{array}{l} \lambda_{tide} = 628 \text{ km} \\ \ell = 1 \text{ m} \\ \text{(tidal difference = 2m)} \end{array}$$

Experiments by OPDAM [13] confirm this theory.

1.4 Longshore velocity

Now we consider a "slice" from the triangular prism mentioned in 1.3. Acting on the bottom is the shear stress, $c_f v$, treated in 1.1. We assume a surging breaker ; in this case the shear stress F_{wave}, mentioned in 1.2 acts on the planes ABCD and A'B'C'D' in opposite direction. This force F_{wave} however, differs on both planes and thus the resultant force equals:

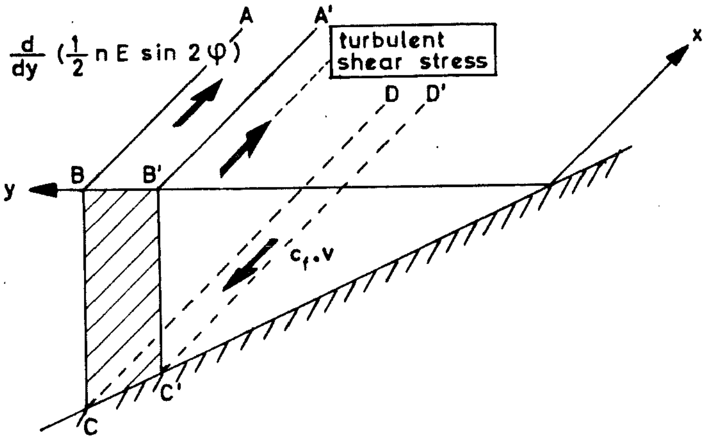

Fig. 6 Stresses on AA' BB' CC' DD'

$$\text{force by waves} = \frac{d}{dy}\left(\tfrac{1}{2}\, n\, E \sin 2\varphi\right) \quad \ldots\ldots\ldots\ldots \quad (19)$$

This resultant force is shown in fig. 6 on the upper plane ABB'A', although it naturally does not work on this plane.
Also acting on the planes ABCD and A'B'C'D' is a turbulent shear force (Reynold stress). BOWEN [2] takes this force into account as a force R_y per unit area:

$$R_y = A_h \frac{d^2 v}{dy^2} \quad \ldots\ldots\ldots\ldots\ldots\ldots \quad (20)$$

A literature review concerning the magnitude of the factor A_h valid in the breaker zone, indicates, that this force is not able to change the distribution of the longshore velocity over the breaker zone significantly (in the prototype).

In the stationary case all the longshore forces have to be in equilibrium. Neglection of the turbulent shear stress R_y leads to:

$$c_f\ v = \frac{d}{dy}\left(\tfrac{1}{2}\ nE\ \sin 2\varphi\right)$$

$$v = \frac{1}{c_f}\cdot\frac{d}{dy}\left(\tfrac{1}{2}\ nE\ \sin 2\varphi\right) \quad \ldots\ldots\ldots\ldots\ldots \quad (21)$$

Substitution of (5) and taking n=1 in the breaker zone:

$$v = \frac{\pi\sqrt{8}}{pK\ A_2}\cdot\frac{1}{\rho\sqrt{fgD}}\cdot\frac{d}{dy}\left(E\ \sin\varphi\cos\varphi\right) \quad \ldots\ldots\ldots\ldots \quad (22)$$

In the case of parallel depth contours in the breaker zone, this can be written more simply.
In the breaker zone φ is mostly small and therefore the approximation $\cos\varphi \approx \cos\varphi_{br}$ is good and $\cos\varphi \approx 1$ sufficiently accurate.
With respect to $\sin\varphi$, Snell's law can be applied.

$$\sin\varphi = \frac{C}{C_{br}}\sin\varphi_{br} = \sqrt{\frac{D}{D_{br}}}\sin\varphi_{br} \quad \ldots\ldots\ldots\ldots \quad (23a)$$

This is a better approximation than BOWEN [2] applies: he takes $\varphi \approx \varphi_{br}$ in the breaker zone.

Using (7) and Snell's law:

$$E\ \sin\varphi\ \cos\varphi \approx \frac{1}{8}\rho g\ H^2 \sin\varphi\ \cos\varphi_{br}$$

$$\frac{1}{8}\rho g\ A_2^{\ 2}D^2\ (D/D_{br})^{\frac{1}{2}}\sin\varphi_{br}\ \cos\varphi_{br}$$

$$E\ \sin\varphi\ \cos\varphi \approx \frac{1}{8}\rho g\ A_2^{\ 2}D^{2\frac{1}{2}}D_{br}^{\ -\frac{1}{2}}\sin\varphi_{br}\ \cos\varphi_{br}$$

$$\frac{d}{dy}\left(E\ \sin\varphi\ \cos\varphi\right) = \frac{d}{dD}\left(E\ \sin\varphi\cos\varphi\right)\frac{dD}{dy}$$

$$\frac{d}{dy}\left(E\ \sin\varphi\ \cos\varphi\right) \approx \frac{5}{16}\rho g\,A_2^{\ 2}D^{1\frac{1}{2}}D_{br}^{\ -\frac{1}{2}}\sin\varphi_{br}\ \cos\varphi_{br}\ tg\alpha_D.$$

in which α_D is the beach slope at depth D. When this slope is negative, α_D is of course zero.

Substituting this result in (22):

$$v = \frac{\pi\sqrt{8}}{pK\,A_2} \cdot \frac{1}{\rho\sqrt{f\,gD}} \cdot \frac{5}{16}\rho g\,A_2{}^2 D^{1\frac{1}{2}}\,D_{br}{}^{-\frac{1}{2}} \sin\varphi_{br} \cos\varphi_{br}\, tg\,\alpha_D$$

$$v = \frac{\pi A_2}{pK} \cdot \frac{5}{16} \cdot \frac{1}{\sqrt{f/8}} \left(\frac{D}{D_{br}}\right)^{\frac{1}{2}} \sqrt{gD}\, \sin\varphi_{br} \cos\varphi_{br}\, tg\,\alpha_D \quad . . . . . (24^a)$$

Substituting $p = .45$, $K = .4$, $\pi = 3.14$:

$$v = 15.44\, A_2 f^{-\frac{1}{2}} g^{\frac{1}{2}}\, D D_{br}{}^{-\frac{1}{2}} \sin\varphi_{br} \cos\varphi_{br}\, tg\,\alpha_D \quad . . . . (24^b)$$

$$v = 5.46\, A_2\, C_h\, D D_{br}{}^{-\frac{1}{2}} \sin\varphi_{br} \cos\varphi_{br}\, tg\,\alpha_D \quad . . . . (24^c)$$ [1)]

2. TRANSPORT FORMULAE

2.1 BIJKER-method

BIJKER [1], [7], [11] assumes, that the waves stir the material and the currents transport it.

The bottom load he computes according to an adapted method of FRIJLINK [14] [1)] and the suspended load according to EINSTEIN [15] or VANONI [16].

2.1.1 Bottom load

The bottom load S_b per m' of coastal profile equals, according to BIJKER:

$$S_b = \text{stream parameter} \cdot e^{-\text{stirring parameter}} \quad . . . . . . (25^a)$$ [2)]

In the surf zone the stirring parameter is proportional to $d_m/\hat{u}$ (approximately), in which d_m is the mean grain diameter. As for sand grains (in prototype circumstances) the stirring parameter is very small and (25) may be simplified to:

$$S_b \approx \text{stream parameter} = A_4\, d_m \sqrt{f/8}\,.\,v \quad . . . . (26)$$

in which $A_4 \approx 5$ according to BIJKER.

---

1) In appendix B the formula, derived here, will be compared with other formulae, based on a momentum approach. Of much importance is appendix C, in which the influence of short-crested waves is considered, as derived by BATTJES.

2) In appendix A the full formulae are given.

2.1.2 Suspended load

Analogous to EINSTEIN, BIJKER states:

$$\frac{S_s}{S_b} = f_1 \left(\frac{\text{depth } D}{\text{ripple height } K}, \frac{\text{fall velocity } w}{\text{shear stress velocity } v_*'} \right) =$$

$$f_1 \left(\frac{D}{K}, \frac{w}{v_*'} \right) \quad . . . . (27)$$

in which S_s is the suspended load and v_*' is the combined shear stress caused by waves and current **and therefore also a function of depth.** [1)]

It is useful to get an impression of the influence of the depth on the ratio between suspended transport and bottom transport and put (27) in the form:

$$\frac{S_s}{S_b} = f \left(\frac{D}{K}, \frac{d_m}{K}\right) \quad . . . . (28)$$

But the influence of viscosity makes a dimensionless plot according to (28) impossible. However, it is possible to plot:

$$\frac{S_s}{S_b} = f_2 \left(\frac{D}{K}, \frac{w}{\sqrt{gK}}\right) \quad . . . . (29)$$

in which w is a function of d_m and viscosity. Assuming that K is constant over the breaker zone (which is questionable) the second parameter is independant of the depth.

The function f_1 from (27) is a known function, given in appendix A. As will be shown also in appendix A, in the case of small value of $v/\hat{u}$, for v_*' can be written:

$$v_*' \approx \frac{pK}{\sqrt{2}} \; \hat{u} \quad . . . . (30)$$

which is curiously enough independant of f.
Thus for w/v_*' can be written, using (6^b):

$$\frac{w}{v_*'} \approx \frac{2\sqrt{2}}{A_2 pK} \cdot \frac{w}{\sqrt{gD}} = \frac{2\sqrt{2}}{A_2 pK} \cdot \frac{w}{\sqrt{gK}} \cdot \sqrt{\frac{K}{D}} \quad . . . . (31)$$

1) In appendix A the full formulae are given

Hence, for given values of D/K and $w/\sqrt{gK}$ according to (29), the corresponding value of w/v_*' can be found from (31) and then, from the given f_1 according to (27) the ratio S_s/S_b can be found. When D/K and $w/\sqrt{gK}$ are known, also S_s/S_b is known (if $v/\hat{u}$ is small).

Annex 2 gives S_s/S_b as a function of D/K for various values of $w/\sqrt{gK}$. The accuracy of the calculation is confined by the accuracy of the graphs of the EINSTEIN integrals I_1 and I_2, mentioned in the appendix.

We may confine ourselves to the region:

$$\left.\begin{aligned} & 10 < D/K < 500 \\ \text{and } & .03 < w/A_2\sqrt{gK} < .15 \end{aligned}\right\} \quad \dots\dots\dots\dots\dots\dots \quad (32)$$

Then for every value of $w/A_2\sqrt{gK}$ as a good fit a straight line can be drawn on double-logarithmic paper, giving the relation between S_s/S_b and the dimensionless depth D/K:

$$\frac{S_s}{S_b} \approx 9.10^4 \left(\frac{D}{1.4.10^4 K}\right)^{1.18 + 0.188.\frac{2\sqrt{2}}{A_2 p K}.\frac{w}{\sqrt{gK}}} \quad \dots\dots\dots \quad (33)$$

Using $A_2 = .78$, $p = .45$, $K = .4$ and within the limits mentioned in (32) this becomes:

$$\frac{S_s}{S_b} \approx 9.10^4 \left(\frac{D}{1.4.10^4 K}\right)^{1.2 \text{ to } 1.6} \quad \dots\dots\dots\dots\dots \quad (34)$$

As can be seen from annex 2 the ratio S_s/S_b is large in the whole region and thus:

$$S \approx S_s \quad \dots\dots\dots\dots\dots\dots\dots\dots\dots \quad (35)$$

From (26), (34), (35):

$$S \approx \frac{9.10^4 A_4}{(1.4.10^4)^{1.2 \text{ to } 1.6}} \left(\frac{D}{K}\right)^{1.2 \text{ to } 1.6} d_m \sqrt{f/8}.v \quad \dots\dots \quad (36)$$

Annex 3 gives as a practical example a comparison between the results of the exact computation according to the BIJKER-method (solid line) and the results according to the approximation of eq.(33) (interrupted line).
The upper figures concern a short-period wave, the lower figures a wave of long period; the left-hand figures concern a shorter wave period than the right-hand figures.
For large values of D and short wave period, deviations occur, because in this case the orbital velocity is not proportional to $\sqrt{gD}$ (no shallow-water wave).
Small values of D and large values of v are not likely to occur simultaneously.

2.2. SVASEK-method (adapted to parallel depth contours)

SVASEK [11] assumes, that the littoral drift between two depth contours is proportional to the longshore component of the loss of energy flux between these depth contours.

Now the energy flux across a depth contour (per unit length of the depth contour) equals EC $\cos\varphi$ and the longshore component EC $\sin\varphi$ $\cos\varphi$. As the energy E is proportional to $\overline{H^2}$, SVASEK finds ([11], formula 5-7):

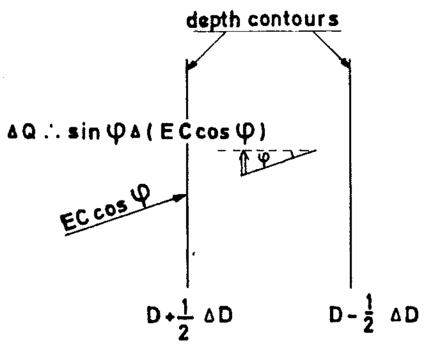

Fig. 7

$$\Delta Q = A_1' . \quad (\overline{H^2}C) \sin\varphi \cos\varphi \quad \ldots\ldots\ldots\ldots\ldots \quad (37)$$

In the breaker zone we may assume:

$$\bar{H} = A_2 D \quad \ldots\ldots \quad (7) \qquad C = A_3 \sqrt{gD} \quad \ldots\ldots\ldots\ldots \quad (38)$$

If the Bernoulli second-order theory for the solitary wave is used, C equals:

$$C = \sqrt{g\ (D + H)}$$

and thus $A_3 = \sqrt{1 + A_2}$

Substituting (7) and (38) in (37) yields for $\Delta(\overline{H^2C})$:

$$\Delta\,(\overline{H^2C}) = \Delta(A_2{}^2 A_3\ g^{\frac{1}{2}} D^{2\frac{1}{2}})$$

$$\Delta\,(\overline{H^2C}) = \tfrac{5}{2}\ A_2{}^2 A_3\ g^{\frac{1}{2}} D^{1\frac{1}{2}}\,\Delta D \ \ldots\ldots\ldots\ldots\ldots \text{(39)}$$

When all contour lines are assumed parallel, we may use Snell's law (23^a), and with the same assumptions as in 1.4 we find:

$$\Delta Q = \tfrac{5}{2}\ A_1{}'\,A_2{}^2 A_3 g^{\frac{1}{2}} D^2 D_{br}{}^{-\frac{1}{2}}\,\Delta D \sin\varphi_{br} \cos\varphi_{br} \ \ldots\ldots \text{(40)}$$

It should be noted, that ΔQ denotes the littoral drift <u>between two depth contours</u>, where S denotes the littoral drift <u>per m' of coastal profile:</u>

$$S = \frac{\Delta Q}{\Delta D}\ \mathrm{tg}\,\alpha_D \ \ldots\ldots\ldots\ldots\ldots\ldots\ldots \text{(41)}$$

Integration of (40) over the surf zone yields:

$$Q = \int_0^{D_{br}} \Delta Q = \tfrac{5}{6}\ \ A_1{}'\,A_2{}^2\ A_3\ g^{\frac{1}{2}}\ D_{br}{}^{2\frac{1}{2}}\ \ \sin\varphi_{br}\ \cos\varphi_{br} \ldots \text{(42)}$$

2.3 <u>CERC-formula.</u>

The formula of the Coastal Engineering Research Center can be written as:

$$Q = 1.4 . 10^{-2}\ H_{sign}^{\ 2}\ C_o\ K_r^{\ 2}\ \sin\varphi_{br}\ \cos\varphi_{br} \ \ldots\ldots \text{(43)},$$

in which K_r is the refraction coefficient and Q the <u>total</u> littoral drift over the surf zone.

Conservation of wave energy between wave rays gives:

$$n_o \overline{H^2} C_o K_r^{\,2} = \overline{H^2_{br}} C_{br} = A_2^{\,2} A_3 g^{\frac{1}{2}} D_{br}^{\,2\frac{1}{2}} \quad \ldots\ldots\ldots\ldots (44)$$

$$H_{sign}^{\,2} C_o K_r^{\,2} = 2\,\overline{H^2} C_o K_r^{\,2} = \frac{2}{n_o} A_2^{\,2} A_3 g^{\frac{1}{2}} D_{br}^{\,2\frac{1}{2}}$$

in which n_o, the ratio between group velocity and phase velocity in deep water, equals $\frac{1}{2}$:

$$n_o = \tfrac{1}{2}$$

Thus: $Q = A_1 A_2^{\,2} A_3 g^{\frac{1}{2}} D_{br}^{2\frac{1}{2}} \sin\varphi_{br} \cos\varphi_{br}$ . . . . (45)

Comparison with (42) shows, that:

$$A_1 = \tfrac{5}{6} A_1' = \frac{2}{n_o} \cdot 1.4 \cdot 10^{-2}$$

$$A_1 = \tfrac{5}{6} A_1' = 5.6 \cdot 10^{-2} \quad \ldots\ldots\ldots\ldots (46)$$

The SVASEK-formula is a variation on the CERC-formula, but it adds an estimation of the distribution of the littoral drift over the surf zone.

2.4 Comparison of the BIJKER- and SVAŠEK-method.

BIJKER [7] uses EAGLESON [5] for the computation of the littoral current; however, it seems an improvement to use the computation of chapter 1.1 and 1.4.

Therefore we substitute v from (22) in the formula (36) for S. A first-sight comparison between BIJKER/BOWEN and SVAŠEK shows:

BIJKER/BOWEN : $S \mathrel{.\!\dot{}\!.} D^{0.7 \text{ to } 1.1} \frac{d}{dy} (E \sin\varphi \cos\varphi)$ . . . . . . (47)

SVAŠEK (fig.7): $S \mathrel{.\!\dot{}\!.} \sin\varphi \frac{d}{dy} (EC \cos\varphi)$ . . . .(48)

The formulae (47) and (48) look quite similar. A more quantitive comparison can be given by the substitution of v from (24) in the formula (36) for S:

BIJKER/BOWEN:

$$S=\left\{\frac{9\cdot 10^4 A_2 A_4}{(1.4\cdot 10^4)^{1.2to1.6}}\cdot\frac{5}{16}\frac{\bar{\pi}}{pK}\left(\frac{D}{K}\right)^{1.2to1.6}\left(\frac{D}{D_{br}}\right)^{\frac{1}{2}} d_m\sqrt{gD}\right\}\cdot\sin\varphi_{br}\cos\varphi_{br}\,tg\alpha_D \ldots (49)$$

SVAŠEK (40), (41), (46)

$$S = 3\, A_1\, A_2^{\,2}\, A_3\, D\left(\frac{D}{D_{br}}\right)^{\frac{1}{2}}\sqrt{gD}\,\sin\varphi_{br}\,\cos\varphi_{br}\,tg\,\alpha_D \ldots\ldots (50)$$

The formulae look quite similar; in (50) $D^{1.2\ to\ 1.6}$ **is replaced** by D. The influence of the ratio $A_2 = \bar{H}/D$ in the breaker zone seems more in the SVASEK-formula than in the BIJKER-formula. However, the influence of A_2 in the BIJKER-formula is also hidden in the exponent "1.2 to 1.6" as (33) shows. BOWEN uses the linear theory, which is the reason, that the factor "A_3" does not occur in (49). The use of the linear theory in SVAŠEK's formula would yield: $A_3 = 1$.

For a better comparison, some numerical values will be substituted in (49) and (50) according to the next table.

assumed data			
A_1	$5.6 \cdot 10^{-2}$	p	.45
A_2	.28 [1]	K	.4
A_3	$\sqrt{1.28}$	d_m	$2 \cdot 10^{-4}$ m
A_4	5	w	$2.4 \cdot 10^{-2}$ m/sec
		K	$3 \cdot 10^{-2}$ m

1) A_2 has been chosen in this way, that $(H_{sign})_{br} = 0.4D$ and $\left(H_{sign}\right)_{br}^{2} = 2\,\overline{H^2}_{br}$, according to SVAŠEK's assumptions.

Computation:

The exponent of D in (33) equals:

$$1.18 + 0.188 * \frac{2\sqrt{2}}{A_2 pK} * \frac{w}{\sqrt{gK}} = 1.18 + 0.188 * \frac{2\sqrt{2}}{0.28*0.45*0.4} * \frac{2.4*10^{-2}}{\sqrt{9.81*0.03}}$$

$$= 1.18 + 0.188*56.0*4.42*10^{-2} = 1.645$$

Thus the coefficient before (49) equals:

$$\frac{9*10^4 A_2 A_4}{(1.4*10^4 K)^{1.645}} * \frac{5}{16} \cdot \frac{\pi}{pK}\, dm = \frac{9*10^4*0.28*5}{(1.4*10^4*3*10^{-2})^{1.645}} * \frac{5}{16} * \frac{\pi}{0.45*0.4} * 2*10^{-4}$$

$$= \frac{12.6*10^4}{2.07*10^4} * 1.09*10^{-3}$$

$$= 6.63*10^{-3}$$

This can be compared with the coefficient before (50):

$$3\, A_1 A_2^2 A_3 = 3*5.6*10^{-2}*0.28^2*\sqrt{1.28} = 15.2*10^{-3}$$

Therefore, in this case the results are comparable when $K \approx 2$ cm and $D \approx 1$ m.

3. MATHEMATICAL COASTAL MODELS [17], [18]

How can we apply this knowledge to the computation of the sedimentation and accretion near groynes and harbour moles?

The construction of groynes has the following effects:

1. Prevention of the littoral sand drift in the area between the coastline and the head of the groyne;
2. Prevention of the longshore current in the same area;
3. Formation of a sheltered area at the lee-side of the groyne caused by diffraction;
4. Changing the wave height by reflection.

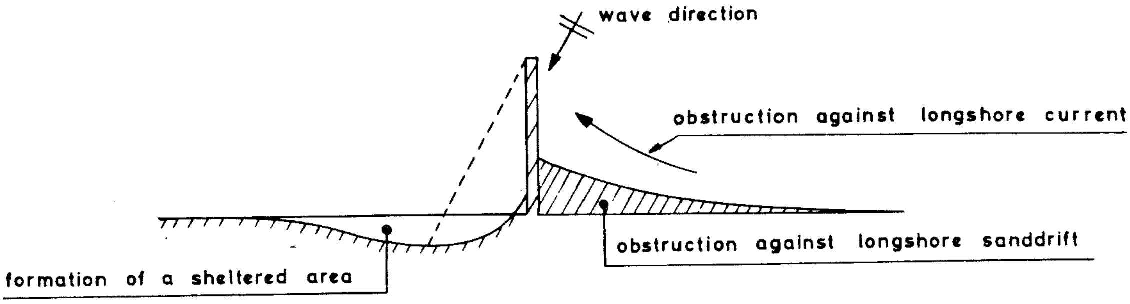

Fig. 8 The effects of the construction of a groyne

The obstruction against sand drift has been treated for the first time by PELNARD-CONSIDÈRE [19].
PELNARD-CONSIDÈRE assumes, that the profile of the coast always remains the equilibrium profile, so that he only needs to consider one coastline, being one of the contour lines. He assumes no tidal currents, constant wave direction, small angle of wave incidence and a linear relation between the angle of wave incidence and the littoral drift.

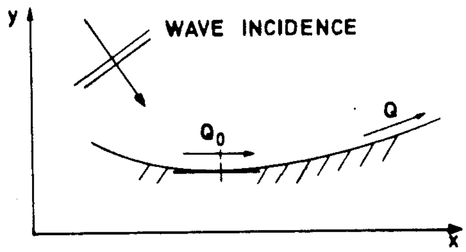

Fig. 9 Littoral drift along the coast

For the littoral drift he assumes:

$$Q = Q_0 - q \frac{\partial y}{\partial x} \quad \ldots\ldots\ldots\ldots\ldots\ldots\ldots\ldots \quad (51)$$

in which:

Q = littoral drift

Q_0 = littoral drift at the point where $\frac{\partial y}{\partial x} = 0$

$q = \frac{dQ}{d\varphi}$ = the derivate of the littoral drift Q to the angle of wave incidence φ.

He finds, that the accretion is proportional to the curvature of the coast:

$$\frac{\partial y}{\partial t} = \frac{q}{D_{tot}} \frac{\partial^2 y}{\partial x^2} \quad \ldots\ldots\ldots\ldots\ldots\ldots\ldots (52)$$

in which D_{tot} is the depth, up to where it is assumed, that sand transport takes place.

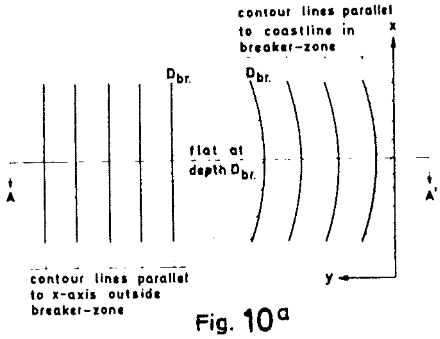

Fig. 10^a

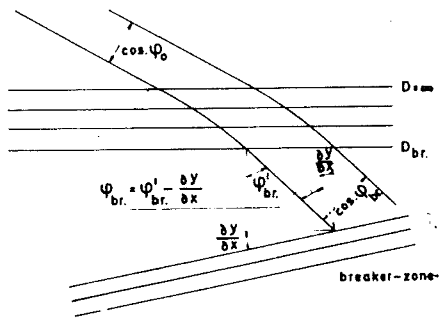

Fig. 10^c

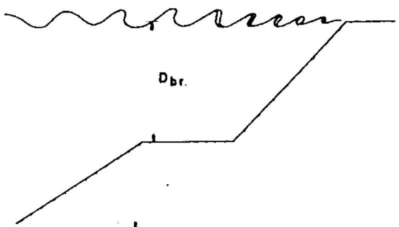

Fig. 10^b Profile A-A'

The constants Q_0 and q can be computed with the SVAŠEK-theory. With the topography according to fig. 10 for Q_0 can be found from (45):

$$Q_0 = A_1 \, A_2^2 \, A_3 \, g^{\frac{1}{2}} \, D_{br}^{2\frac{1}{2}} \sin\varphi'_{br} \, \cos\varphi'_{br} \quad \ldots\ldots\ldots\ldots (53)$$

$$q = A_1 \, A_2^2 \, A_3 \, g^{\frac{1}{2}} \, D_{br}^{2\frac{1}{2}} \cos 2\varphi'_{br} \quad \ldots\ldots\ldots\ldots\ldots\ldots (54)$$

However, if one takes diffraction near a harbour mole into account, the wave height and wave direction change and therefore Q_0 (the transport when the coastline is parallel to the x-axis) and $\frac{dQ}{d\varphi}$ vary in the coastal direction.

I assumed, that the littoral drift is proportional to the square of the wave height and proportional to the angle of wave incidence.

For the calculation of the coastlines a computer program has been developed. Fig. 11 shows the calculated development of a coast with one groyne. Comparison of the interrupted and the solid line gives an impression of the influence of diffraction. The interrupted lines give the erosion according to PELNARD-CONSIDERE.

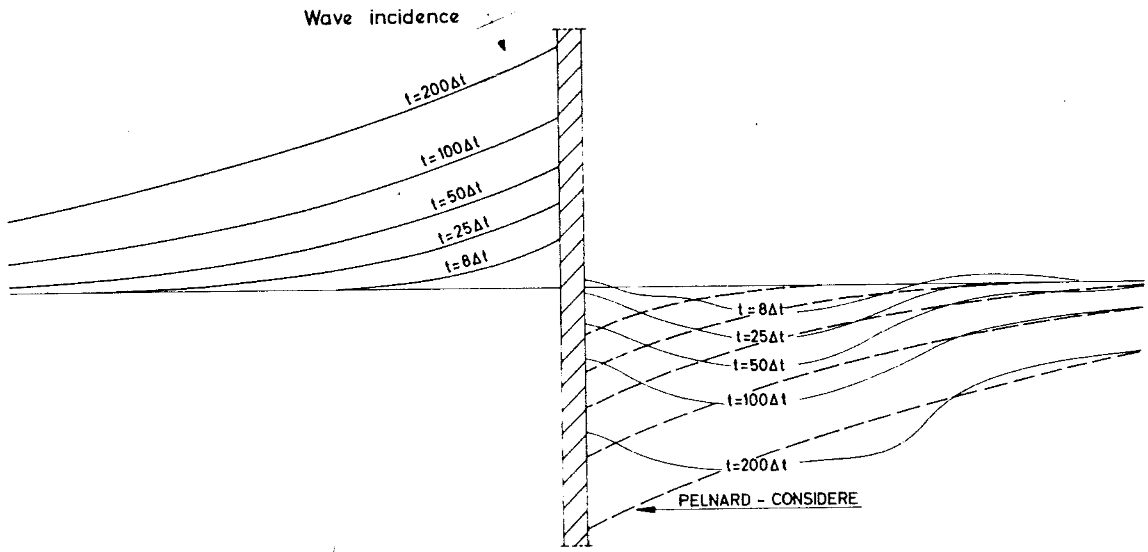

Fig. 11 Accretion and erosion near a groyne, numerical solution with diffraction (one line theory). The dotted lines at the right hand gives erosion according to Pelnard - Considere.

With the computer program we calculated the behaviour of the coastline between two groynes with the influence of diffraction. The result is shown in fig. 12.

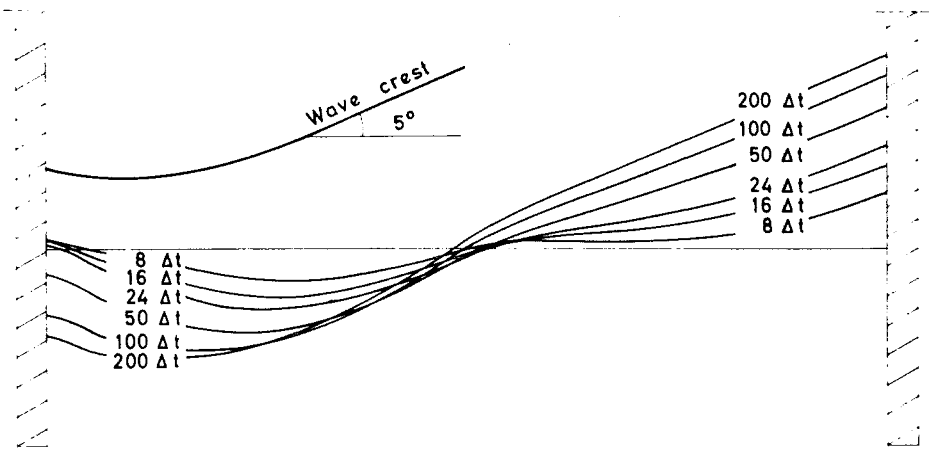

Fig. 12 Behavior of the coastline between two groynes (one-line theory)

An extension of this theory was made, dropping the assumption of an equilibrium profile.

The coast was schematized by two lines, one representing the beach, the other one the inshore. Dependant on the distance between these lines, on- and offshore transport was assumed (fig. 13, fig. 14).
Taking diffraction into account, the development of a coast in case of one groyne and between an infinite row of groynes could be computed.
The results are shown in fig. 15 and 16 respectively.

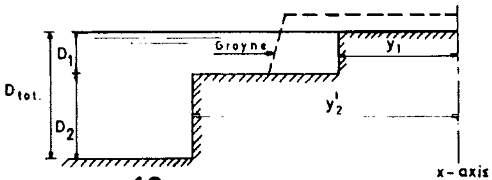

Fig. 13 Schematized profile

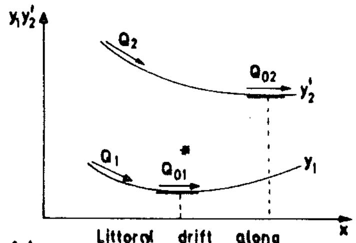

Fig. 14 Littoral drift along beach and inshore

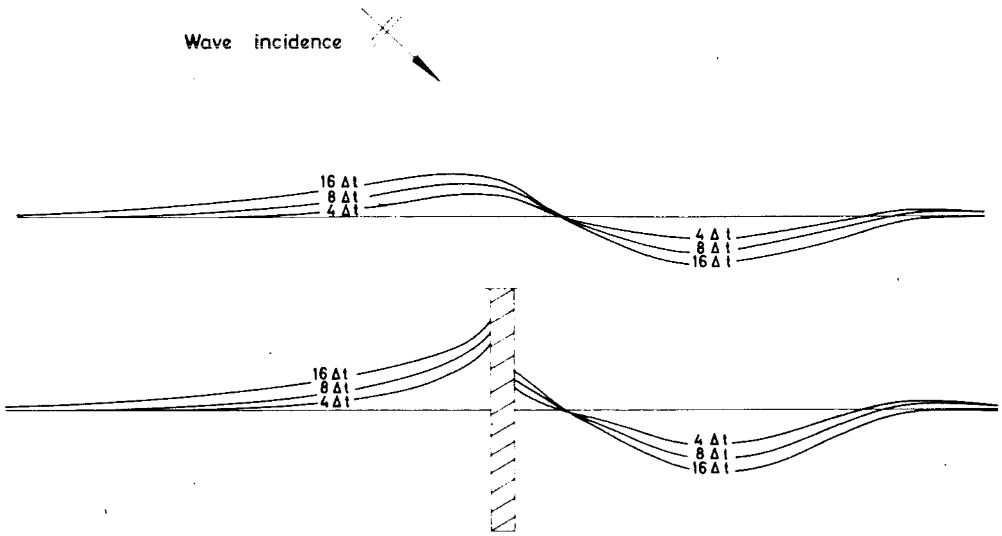

Fig. 15 Accretion and erosion near a groyne, numerical solution with diffraction (two-line theory)

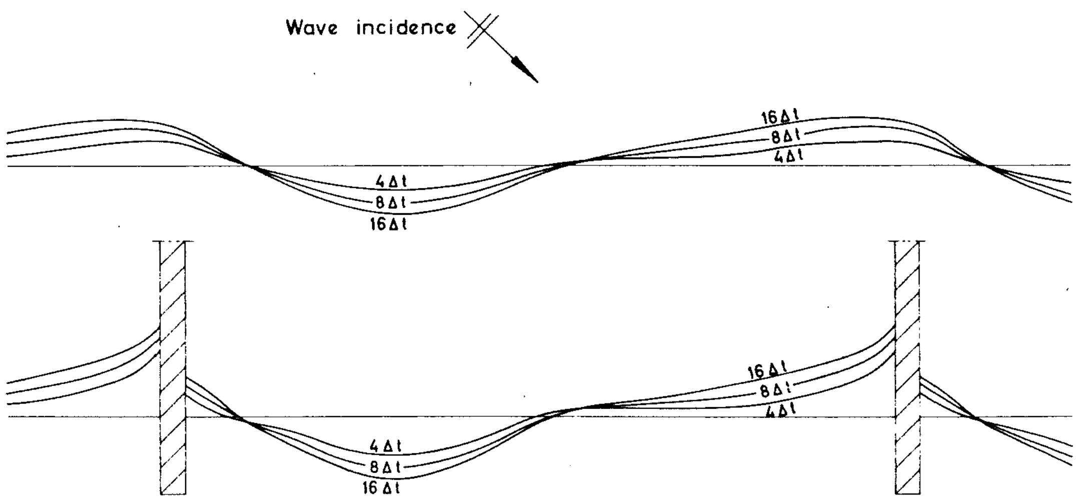

Fig. 16 Behaviour of beach and inshore between two groynes. (two-line theory)

In the annexes 4 and 5 some preliminary results are shown in which the waves come first 25 time steps from one direction and then switch: 50 time steps from the other direction, 50 time steps from the first direction and so on. However, the results are still inaccurate.

Annex 4 shows the development of a coast near 1 groyne and annex 5 between two groynes. The vertical scale is 5 times exaggerated with respect to the horizontal scale.

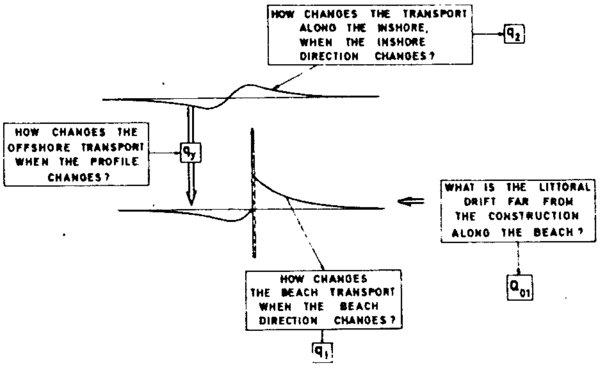

Fig. 17

For this solutions the following variables have to be known (fig.17).

1° The littoral drift Q_0, along the beach, far from the construction

2° The change of the littoral drift along the beach, when the beach direction changes: $q_1 = \frac{dQ_{01}}{d\varphi}$

3° The change of the littoral drift along the inshore, when the inshore direction changes: $q_2 = \frac{dQ_{02}}{d\varphi}$

4° The change in offshore transport when the profile changes.

Little is yet known about the last-mentioned variable, although preliminary research has already been done.

The coefficients Q_{01}, q_1, Q_{02} and q_2 are computed with the SVAŠEK-theory in [20] . Assuming a topography according to fig. 18, one finds the following results, valid for small angle of wave incidence:

$$S_{01} = A_1\, A_2^{\,2}\, A_3\, g^{\frac{1}{2}}\, D_1^{\,3}\, D_{br}^{\,-\frac{1}{2}} \sin \varphi'_{br} \quad \ldots\ldots\ldots \quad (55)^{1)}$$

$$q_1 = A_1\, A_2^{\,2}\, A_3\, g^{\frac{1}{2}}\, D_1^{\,2\frac{1}{2}} \quad \ldots\ldots\ldots\ldots\ldots \quad (56)$$

$$S_{02} = A_1\, A_2^{\,2}\, A_3\, g^{\frac{1}{2}}\, (D_{br}^{\,3} - D_1^{\,3})\, D_{br}^{\,-\frac{1}{2}} \sin \varphi'_{br} \quad \ldots \quad (57)$$

$$q_2 = A_1\, A_2^{\,2}\, A_3\, g^{\frac{1}{2}}\, (D_{br}^{\,3} - D_1^{\,3})\, D_{br}^{\,-\frac{1}{2}} \quad \ldots\ldots\ldots\ldots \quad (58)$$

It must be stressed that up to now only the obstruction against longshore sand-drift and the formation of a sheltered area has been investigated.
In the future, the effect of the obstruction of the longshore current with its effects as entrainment of littoral drift to the inshore and formation of a scour hole in front of the groyne will be investigated, as well as the variation of the set-up near the groyne because of changing wave conditions.

Some preliminary research in this field has already been done.

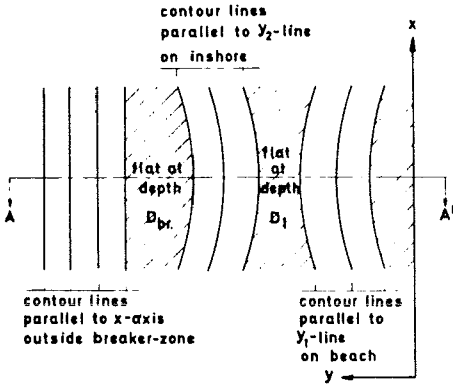

Fig 18^a Upper view

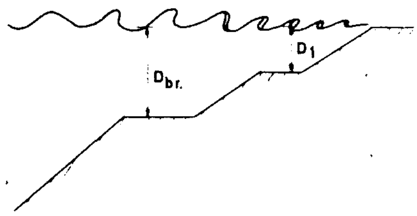

Fig 18^b Profile A-A'

---

1) φ'_{br} is the angle of the wave crest with the x-axis, when the waves enter on the flat at depth D_{br} (fig. 10^c)

APPENDIX A

FRIJLINK formula

The following text has been rewritten from BIJKER [7], page 2. The notation has been adapted.

"Most bed load formulae may be written in the form:

$$\frac{S_b}{f(d\ g^{\frac{1}{2}}\Delta)} = f\left(\frac{\Delta d}{\mu DI}\right) \qquad \dots\dots\dots\dots\dots\dots\dots \text{(A1)}$$

in which Δ = relative apparent density, d = grain size, D = water depth, I is energy gradient, μ = ripple coefficient[1] and g = acceleration of gravity.

FRIJLINK [14] suggested, starting from the formula of Kalinske, to write formula (A1) in the following way:

$$\frac{S_b}{d(\mu\tau/\rho)^{\frac{1}{2}}} = b\ e^{a\frac{\Delta d \rho g}{\mu \tau}} \qquad \dots\dots\dots\dots\dots\dots \text{(A2)}$$

where C_h resistance coefficient and τ = bed shear $= \rho g DI = \rho g\ v^2/C_h^2$."

In an earlier paper BIJKER [1] called the first term the transport parameter and the exponent of e in the second term the stirring parameter[1].

BIJKER formula

BIJKER [1] replaces in (A2) the shear stress τ_c by the mean resultant bed shear τ_r of the combination of waves and current:

$$\tau_r = \left[1 + \tfrac{1}{2}\left(\xi\frac{u_o}{v}\right)^2\right]\tau_c \qquad \dots\dots\dots\dots\dots\dots\dots \text{(A3)}$$

in which $\xi = pK\,C_h/\sqrt{g}$ $\qquad \dots\dots\dots\dots\dots\dots\dots\dots \text{(A4)}$

The shear stress velocity $v_* = \sqrt{\tau_c/\rho} = v\sqrt{g}/C_h$ is thus replaced by:

$$v_*' = \frac{v}{C_h}\sqrt{g}\left\{1 + \tfrac{1}{2}\left(\xi\frac{u_o}{v}\right)^2\right\}^{\frac{1}{2}} \qquad \dots\dots\dots\dots\dots\dots \text{(A5)}$$

---

1) Usually the ripple factor μ is taken as $\mu = (C_h/C_h')^{3/2}$, in which

$C_h' = 18 \log 12\ D/d$ and

$C_h = 18 \log 12\ D/k$

Substitution of (A3) in (A2) yields:

$$S_b = A_4 \ d \ v \sqrt{g/C_h^2} \quad e^{-0.27 \frac{\Delta d \ C_h^2}{\mu v^2 \left\{1+\frac{1}{2}(\xi \frac{u_o}{v})^2\right\}}} \quad \ldots\ldots\ldots (A6)$$

The factor A_4 should be choosen ≈ 5, according to BIJKER.
With respect to the suspended load BIJKER assumes that the bottom load is transported in a layer immediately above the bed with a thickness equal to that of the fictiteous bed roughness K, from which ([7], page 9) as mean concentration C_K in this bottom layer is found:

$$C_K = S_b \ / \ \bar{v}_{o-r} = S_b \ / \ 6.35 \ v_*' K \quad \ldots\ldots\ldots\ldots (A7)$$

Furthermore BIJKER uses EINSTEIN [15], except that he changes the factor " 11.6 c_a v_* a" of EINSTEIN into $\frac{11.6}{6.35}$ S_b = 1.83 S_b according to (A7):

$$S_s = 1.83 \ \ S_b \left[I_1 \ln 33 \ D/K + I_2 \right]^{1)} \quad \ldots\ldots\ldots\ldots (A8)$$

in which I_1 and I_2 are the EINSTEIN-integrals:

$$I_1 = .216 \frac{(\frac{K}{D})^{z-1}}{(1-\frac{K}{D})^z} \int_{K/D}^{1} (\frac{1-y}{y})^z \ dy \quad \ldots\ldots\ldots\ldots (A9)$$

$$I_2 = .216 \frac{(\frac{K}{D})^{z-1}}{(1-\frac{K}{D})^z} \int_{K/D}^{1} (\frac{1-y}{y})^z \ \ln y \ dy \quad \ldots\ldots\ldots (A10)$$

in which $z = w/K \ v_*'$
The values of the integrals can be found from graphs in the paper of EINSTEIN, giving I_1 and I_2 respectively as a function of K/D and z.

1) cp. EINSTEIN: $S_s = 11.6 \ c_a \ v_* \ a \left[I_1 \ \ln 33 \ D/K + I_2\right]$, c_a being concentration in bottom layer with tichness a.

Reduction of the BIJKER-formula for small values of v/u_o

For small values of v/u_o (A5) can be reduced in the following way:

$$v_*' = \frac{\sqrt{g}}{C_h} \left\{ v^2 + \tfrac{1}{2} (\xi u_o)^2 \right\}^{\frac{1}{2}}$$

Neglection of v with respect to ξ u_o (in which ξ is about 3):

$$v_*' = \frac{\sqrt{g}}{C_h} \cdot \frac{1}{\sqrt{2}} \cdot \frac{p K C_h}{\sqrt{g}} u_o$$

(A4) has been used.

$$v_*' = \frac{p K}{\sqrt{2}} \hat{u}$$

according to (30).

APPENDIX B [1)]

COMPARISON LONGSHORE-CURRENT FORMULAE

In this appendix the longshore-current formula (24) with its evaluation will be compared with other longshore-current formulae.

As noted by GALVIN [24] , equations to predict longshore current velocity can be grouped into three classes, according to the predominant theory as follows: (1) conservation of momentum; (2) conservation of mass; (3) emperical correlation of data.

The developed theory falls in the first category and in order to show it in its content it is sufficient to consider only the most important theories in this category:
EAGLESON [5] , PUTNAM, MUNK and TRAYLOR [4] , LONGUET HIGGINS [21] .

B1. Comparison EAGLESON and BAKKER

We shall now compare the EAGLESON - approach [5] for computation of the longshore current with the approach developed in the present report which results in (24).

1. EAGLESON investigates the growth of a longshore current, i.e. he allows a variation of the longshore current in coastal direction (= x-direction). This is more sophisticated than the present theory. So we have to compare the limiting uniform, fully-developed current of EAGLESON with the present solution.
2. EAGLESON assumes a uniform distribution of $u \sin\varphi$ (i.e. the longshore component of the water velocity) in the surf zone in y-direction for any value of x and t. He thus assumes that the longshore current in the breaker zone is no function of y.
   In the present theory it has been shown, that both u and $\sin\varphi$ vary with $\sqrt{D/D_{br}}$, and thus $u \sin\varphi$ varies with D/D_{br}.
3. In fig B1 the variations of the longshore component of the water velocity according to EAGLESON and according to the present theory are shown.

---
1) appendix B and C are composed July, 1971.

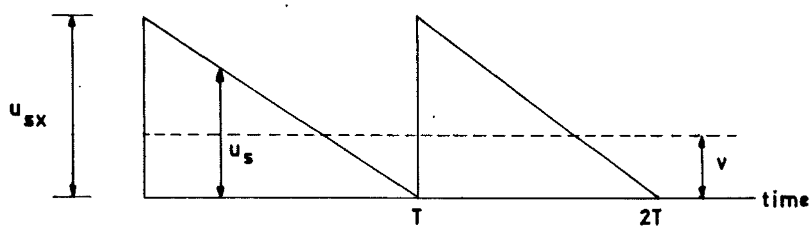

Fig. B 1[a] Variations in longshore water velocity u sin.φ according to EAGLESON

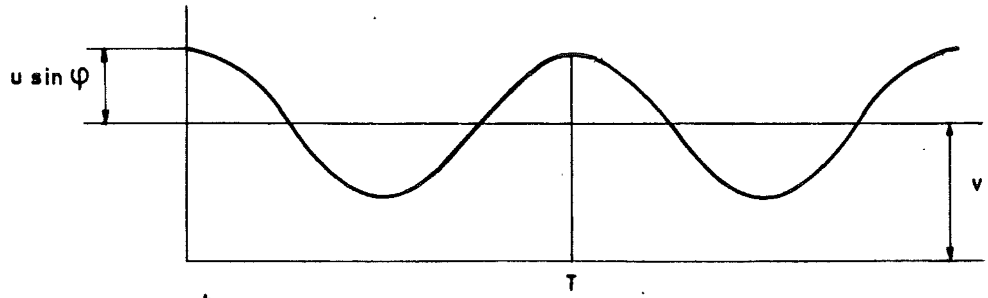

Fig. B 1[b] Variations in longshore water velocity u sin φ according to BAKKER

4. EAGLESON assumes a bottom friction equal to $\rho f\, u_s^{\,2}/8$ (fig. B 1[a]); averaged over time and over the whole breaker zone, this gives a total friction force over the breaker zone (cf EAGLESON formula 3.18):

$$\text{friction force} = 1/6\ \frac{D_{br} \cdot f \sec\alpha}{m \sin\varphi} \cdot \rho v^2$$

Per unit of mass, this gives a force, in the opposite direction to the longshore current, equal to:

$$\text{friction force per unit of mass} = \frac{D_{br}\ f/6\ m \sin\varphi}{D_{br}^{\,2}\ /\ 2\ m} \cdot v^2$$

$$\text{friction force per unit of mass} = \frac{f}{3} \cdot \left[\frac{v^2/\sin\varphi}{D_{br}}\right] \qquad \ldots\ldots\ldots \text{(B1)}$$

Compare the present report, (3):

$$\frac{\overline{\tau}_{\text{longshore}}}{\rho D} = \frac{2}{\pi}\, p K \sqrt{\frac{f}{8}} \cdot \left[\frac{\hat{u}\ v}{D}\right] \qquad \ldots\ldots \text{(B2)}$$

Note the difference between D and D_{br} in (B1) and (B2); in (B1) $\varphi = \varphi_{br}$.

Mind, that in (B2) $\hat{u}$ is proportional to $\sqrt{gD}$ and v is found to be proportional to D.

The formulae (B1) and (B2) have the same construction. The bracketed sections are more or less similar, but EAGLESON takes the friction force proportional to $v^2/\sin\varphi$ instead of uv. The coefficients outside the brackets have the same order of magnitude:

taking f = .03, the coefficient in (B1) equals .01 and in (B2) it is:

$$\frac{2}{\pi} p K \sqrt{\frac{f}{8}} = \frac{2*0.4*0.45}{3.14}\sqrt{\frac{0.03}{8}} = 0.007$$

5. The total generating force of the longshore current is in both cases the same; i.e. the impulsive force in longshore direction of the waves.

However, EAGLESON distributes the force uniformly over the volume of the surf zone; in this report on the other hand the force per unit of mass appears to be proportional to:

$$\frac{d\,(E \sin\varphi)}{dD} \cdot \frac{1}{D} \therefore \frac{d\,(D^{2\frac{1}{2}} \sin\varphi_{br})}{dD} \cdot \frac{1}{D} \therefore D^{\frac{1}{2}}$$

6. The resulting longshore velocity.

Taking $\sin\alpha \approx m$, $n_b = 1$ and $\cos\varphi_b \approx 1$, EAGLESON finds:

$$v = A_2 \sqrt{\frac{3}{4} m \cdot \frac{gD_{br}}{f}} \cdot \sin\varphi_{br}$$

instead of (24):

$$v = 15.44\ A_2 m \sqrt{\frac{gD_{br}}{f}} \cdot \frac{D}{D_{br}} \sin\varphi_{br}$$

Summarizing:

EAGLESON takes the influence of the bottom slope m too small and a uniform instead of a triangular distribution of the velocity over the surf zone.

He takes the bottom friction proportional to $v^2/\sin\varphi$ instead of proportional to uv. However, the factor $v^2/\sin\varphi$ still gives a considerable increase of shear stress, in relation to the v^2, used by PUTNAM, MUNK and TRAYLOR (cf B2).

We shall now consider the difference in the numerical values of the longshore velocity according to BAKKER and EAGLESON respectively.

$$\frac{\overline{v}_{BAKKER}}{v_{EAGLESON}} = \frac{\frac{1}{2} \times 15.44}{\sqrt{\frac{3}{4}}} \sqrt{m}$$

$\overline{v}_{BAKKER}$ denotes the mean velocity in the surf zone = $\frac{1}{2}$ x maximum velocity.

$$\frac{\overline{v}_{BAKKER}}{v_{EAGLESON}} = 8.9 \sqrt{m} \qquad \text{(B3)}$$

The next table gives the value of this relation for various values of m.

m	$\overline{v}_{BAKKER}$ / $\overline{v}_{EAGLESON}$
1:10	2.8
1:20	2.0
1:50	1.26
1:100	0.89

For steep slopes the assumption of BAKKER, that the turbulent shear stress can be neglected, will not be valid and thus the longshore velocities will be too high in that case.

B2. Comparison between PUTNAM, MUNK and TRAYLOR and BAKKER

Another momentum approach is from PUTNAM, MUNK and TRAYLOR (1949) [4]. Differences with the BAKKER computations are:

1. PUTNAM c.s. assume a uniformly distributed longshore current velocity v in the surf zone.
2. A different momentum flow is assumed.
   It is assumed, that the inflow of water in the breaker zone has a longshore component of its velocity equal to C sin φ, and that the outflow of the water from the surf zone takes place with a longshore

velocity component v, thus giving an excess of momentum equal to:

flux of momentum per unit length
in longshore direction $= (C \sin\varphi - v) \rho F \cos\varphi / T$,

F being the cross-sectional area of a breaking wave crest.

3. It is of crucial importance, that PUTNAM c.s. use the solitary wave theory instead of the linear wave theory, thus assuming, that after each wave there elapses some time without waves, in which time the surplus of water in the surf zone has the opportunity to flow back out of the surf zone (with longshore velocity v). They assume a solitary wave of maximum wave height, being 0.78 D (which is correct, **MacCOWAN** [22]) and a wave velocity $C = \sqrt{g\ (D + H)} = \sqrt{1.78 gD}$ (which is not correct; should be $\sqrt{1.56 gD}$ according to MacCOWAN, as the formula $C = \sqrt{g(D+H)}$ only holds for low solitary waves).

As F equals (MUNK [23]):

$$F = 4\ D^2 \sqrt{A_2/3},$$

they find for the flux of momentum:

$$\text{flux of momentum} = 4\sqrt{0.78/3}\ \ (\rho D^2/T).(\sqrt{2.28\ gD}\ \sin\varphi - v)\ \cos\varphi\ .$$

To get an impression of the order of magnitude, we neglect v for a while:

$$\text{flux of momentum} \approx 4\sqrt{\frac{2.28 \times 0.78}{3}}\ \rho g^{\frac{1}{2}}\ D_{br}^{2\frac{1}{2}}\ T^{-1}\ \ \sin\varphi \cos\varphi$$

$$\text{to compare with } 1/8\ \rho g H^2 \sin\varphi \cos\varphi = 1/8\ \ A_2^{\ 2}\ \rho g\ D_{br}^{\ 2}\ \ \sin\varphi \cos\varphi$$

Taking in the second case also $A_2 = 0.78$, the ratio between the fluxes equals:

$$\frac{\text{flux}_{\text{PUTNAM et al}}}{\text{flux}_{\text{EAGLESON et al}}} = \frac{32}{(0.78)^{3/2}} \times \left(\frac{2,28}{3 \times 2\pi}\ \ \frac{D_{br}}{L_o}\right)^{\frac{1}{2}}$$

$$\frac{\text{flux}_{\text{PUTNAM et al}}}{\text{flux}_{\text{EAGLESON et al}}} = 16,5\ \sqrt{\frac{D_{br}}{L_o}} \qquad \text{. . . . . (B4)}$$

4. PUTNAM et al assume the frictional force per unit mass:

$$\text{frictional force per unit of mass} = \frac{f}{8} \cdot \frac{v^2}{D_{br}} \qquad \text{(B5)}$$

to compare with (B1) and (B2).
However it must be stated, that PUTNAM et al replace "f/8" by a factor "K" without mentioning the relation between K and the DARCY-WEISBACH friction coefficient.
As can be expected, they find rather high values for "K" (about 3 to 40 times the expected values, cf EAGLESON [5], table I).

B3. Comparison LONGUET-HIGGINS [21] and BAKKER

LONGUET-HIGGINS finds as formula for the littoral current in the surf zone (in case of absence of horizontal mixing) (cf (55) of [21]):

$$v = \frac{5\pi}{16} \frac{A_2}{f/8} \left(\frac{D}{D_{br}}\right)^{\frac{1}{2}} \sqrt{gD} \sin\varphi_{br} \operatorname{tg}\alpha \qquad \text{(B6)}$$

to compare with (24):

$$v = \frac{5\pi}{16} \frac{A_2}{pK\sqrt{f/8}} \left(\frac{D}{D_{br}}\right)^{\frac{1}{2}} \sqrt{gD} \sin\varphi_{br} \cos\varphi_{br} \operatorname{tg}\alpha \qquad \text{(24)}$$

The formulae are very similar; indepently both authors came to nearly the same conclusions.[2] As for neglection of $\cos\varphi_{br}$ by LONGUET-HIGGINS, the most important difference is the factor:

$$\frac{\sqrt{f/8}}{pK},$$

which orginates in the assumptions of friction according to BIJKER.

---

1) In this formula the notation has been adapted: "α" $\rightarrow A_2/2$; "C" $\rightarrow f/8$; "h" $\rightarrow$ D; s $\rightarrow \operatorname{tg}\alpha$

2) At the time of the lecture in the Hydraulic Res. Station and during the writing of the manuscript the paper of Longuet-Higgins was not known to the author.

APPENDIX C

SHORT CRESTED WAVES

According to a private communication of BATTJES the kind of wave, which generates the longshore current, is of crucial importance. In the afore-mentioned approach it is assumed, that the waves were long-crested; however, in the prototype, short-crested waves can be expected.

Citing BATTJES:

"The surface elevation is supposed to be the result of the superposition of a large number of long-crested progressive sinusoidal component-waves in random phase (Longuet-Higgins, 1957). A two-dimensional energy spectrum $G(\omega, \Theta)$ is defined for wave frequency $\omega \geqslant 0$ and wave direction $|\Theta| \leq \pi$ such that the component-waves with angular frequency in the interval $(\omega, \omega + \partial\omega)$ and direction of propagation in the interval $(\Theta, \Theta + \partial\Theta)$ together contribute an amount $G(\omega, \Theta)\partial\omega\,\partial\Theta$ to the total variance of the water surface η. For convenience, $G(\omega, \Theta)$ is factorized as follows:

$$G(\omega, \Theta) = H(\omega)\; f(\Theta, \omega) \qquad \text{(C1)}$$

such that:

$$\int_{-\pi}^{\pi} f(\Theta, \omega)\, d\Theta = 1 \qquad \text{(C2)}$$

$H(\omega)$ is the energy frequency spectrum, $f(\Theta, \omega)$ gives the angular distribution of the energy.

The average energy content of the waves per unit area is given (to second order) by

$$\underline{E} \approx \rho g \overline{\eta^2} = \rho g \int_0^{\infty}\int_{-\pi}^{\pi} G(\omega, \Theta)\, d\omega d\Theta = \rho g \int_0^{\infty} H(\omega)\, d\omega \qquad \text{(C3)}$$

So far BATTJES. [1)]

Several authors (PIERSON, 1955, COTE et al (SWOP), 1960, KRYLOV et al) have investigated the function $f(\Theta, \omega)$.

---

1) BATTJES continues by investigating the influence of the various assumptions about $f(\Theta, \omega)$ on the radiation stress more generally and more thoroughly than done here.

We shall investigate the influence of the shear stress, making use of the simple assumption of PIERSON [25] about $f(\Theta, \omega)$ in which $f(\Theta, \omega)$ is not even a function of ω:

$$f = \frac{2}{\pi} \cos^2 \Theta \qquad \text{(C4)}$$

Assume $\Theta = 0$ for the mean wave direction φ.
The component waves with wave direction Θ with respect to φ give a shear stress equal to:

$$\tau = \tfrac{1}{2}\, nE \sin 2\,(\varphi - \Theta) \qquad \text{(C5)}$$

Thus the total shear force changes to a kind of "mean value":

$$\tau = \int_{-\pi/2}^{\pi/2} \tfrac{1}{2}\, nE \left\{ \sin 2\,(\varphi - \Theta) \right\} f\,(\Theta)\, d\Theta \qquad \text{(C6)}$$

Using (C5)

$$\bar{\tau} = \tfrac{1}{2}\, nE \,.\, \frac{2}{\pi} \int_{-\pi/2}^{\pi/2} \sin 2\,(\varphi - \Theta) \cos^2 \Theta\, d\,\Theta \qquad \text{(C7)}$$

$$\bar{\tau} = \tfrac{1}{2}\, nE \,.\, \frac{1}{\pi} \int_{-\pi/2}^{\pi/2} \sin 2\,(\varphi - \Theta)\,(1 + \cos 2\,\Theta)\, d\Theta$$

$$\bar{\tau} = \tfrac{1}{2}\, nE \,.\, \frac{1}{\pi} \left[-\tfrac{1}{2} \cos 2\,(\varphi - \Theta) \Big|_{-\pi/2}^{\pi/2} + \int_{-\pi/2}^{\pi/2} (\sin 2\varphi \cos 2\Theta - \cos 2\varphi \sin 2\Theta) \cos 2\Theta\, d\Theta \right]$$

$$\bar{\tau} = \tfrac{1}{2}\, nE \,.\, \frac{1}{\pi} \left[\sin 2\varphi \int_{-\pi/2}^{\pi/2} \cos^2 2\Theta\, d\Theta \right]$$

$$\bar{\tau} = \tfrac{1}{2}\, nE \sin 2\varphi \,.\, \frac{1}{\pi} \,.\, \frac{\pi}{2}$$

$$\bar{\tau} = \tfrac{1}{4}\, nE \sin 2\varphi$$

Conclusion:

$\bar{\tau}$ IS HALF THE VALUE OF τ, OCCURRING WITH LONG-CRESTED WAVES!

The same result was obtained earlier and more general by BATTJES [27].

LIST OF SYMBOLS

A_1	coefficient in (46): ratio between littoral drift and longshore component of wave energy flux.
A_1'	coefficient in (37) (Svašek formula)
A_2	ratio between $\bar{H}$ and D (7)
A_3	Froude number: ratio $C/\sqrt{gD}$
A_4	coefficient in BIJKER-formula (A6)
A_h	turbulence coefficient in (20)
c_a	concentration of sediment in bottom layer (with height $a \approx 2d$)
c_f	coefficient of bottom friction = τ_{bottom}/v
C	celerity of wave propagation
C_h	Chezy coefficient
d_m	mean grain diameter
D	water depth
D_1	depth of beach area (fig. 13)
D_2	depth of inshore area (fig. 13)
D_{tot}	$= D_1 + D_2$
D_{br}	breaker depth
E	wave energy per unit of area
F_{wave}	shear force per unit of length, integrated over the depth (component S_{xy} of radiation stress tensor)
F_{tide}	tidal force per unit of length, integrated over the depth.
f	Darcy-Weisbach friction coefficient
g	acceleration of gravity
h	tidal elevation above the mean water level

H	wave height
$\bar{H}$	mean wave height
H_{br}	breaker wave height
K	ripple height
K_r	refraction coefficient
m	bottom slope
n	ratio group-/fase velocity
p	constant, indicating the ratio between the orbital bottom velocity according to the linear theory and the orbital velocity, significant for the shear stress cf [1], chapter III. 5.
p	in eq (9): water pressure
$\bar{p}$	mean water pressure (averaged over a wave period)
q	derivative of Q to φ (indicating how much the littoral drift changes when the wave direction changes)
q_1	derivative of Q_1 to φ_1
q_2	derivative of Q_2 to φ_2
Q	littoral drift along the coast
Q_1	littoral drift along the beach
Q_2	littoral drift along the inshore
Q_0	littoral drift along the coast, when the coast is parallel to the x-axis
Q_{01}	littoral drift along the beach when the beach is parallel to the x-axis
Q_{02}	littoral drift along the inshore when the inshore is parallel to the x-axis
S_b	bottom transport per unit of time and length, integrated over the depth

S_s	suspended transport per unit of time and length, integrated over the depth
u	orbital velocity
$\hat{u}$	maximum orbital velocity
v	longshore velocity
v_*	shear stress velocity
v_*'	shear stress velocity, including the effect of orbital velocity (A5)
v_n	velocity component in a direction normal to a certain plane
w	still water, fall velocity
x	abcissa, in mean longshore direction
y	ordinate, in seaward direction (perpendicular to x-direction)
z	$w/K \times v_*'$
$\hat{z}$	amplitude of a tidal wave
Δ	relative apparent density
η	wave elevation above mean water level
K	constant of von Karman
μ	ripple coefficient
ξ	$pK\, C_h / \sqrt{g}$
ρ	specific density
φ	angle of wave incidence
φ_{br}	breaker angle
τ	shear stress
$\tau_{longshore}$	longshore component of the shear stress
ω	wave frequency

LIST OF LITERATURE

[1] Bijker, E.W.
Some considerations about scales for coastal models with movable bed.
D. Sc. - Thesis, Techn. Univ. Delft, 1967.

[2] Bowen, A.J.
The generation of longshore currents on a plane beach.
Journal of Marine Research 27, p 206-215, 1969.

[3] Longuet-Higgins, M.S.
On the statistical distribution of the heights of sea waves.
Journal of Marine Research 11, p 245-266, 1952.

[4] Putnam, J.A., Munk, W.H. and Traylor, M.A.
The prediction of longshore currents.
Trans. A.G.U. 30, p 337-345, 1949.

[5] Eagleson, P.S.
Theoretical study of longshore currents on a plane beach.
M.I.T. Dept. of Civ. Eng., Hydr. Lab. Rep. nr. 82, 1965.

[6] Galvin, C.J. and Eagleson, P.S.
Experimental study of longshore currents on a plane beach.
U.S. Army, Coastal Eng. Res. Center, Techn. Memo 10, 1965

[7] Bijker, E.W.
Littoral drift as a function of waves and current.
Publ. 58 Delft Hydraulic Laboratory.

[8] Longuet-Higgins M.S. and Stewart R.W.
Radiation stress and mass transport in gravity waves.
J. Fluid Mech. 13, p 481-504, 1962.

[9] Longuet-Higgins M.S. and Stewart R.W.
Radiation stresses in water waves: a physical discussion with applications.
Deep Sea Res. 11, p 529-562, 1964.

[10] Bakker W.T. and Opdam H.J.
Over de invloed van golven en getij op het zandtransport in de brandingszone (The influence of waves and tides on the sand transport in the surf zone).
Rijkswaterstaat, Dir. for Hydr. Res., Dept. for Coastal Res., Study report W.W.K. 70-9.

[11] Bijker E.W. and Svašek J.N.
Two methods for the determination of morphological changes induced by coastal structures.
XXIInd Int. Nav. Congress, section II item 4, Paris 1969.

[12] Bruyn, P.A. de
Mond Haringvliet.
Golfhoogte frequentie krommen met analystische beschouwing.
Rijkswaterstaat, Waterloopk. Afd. Hellevoetsluis (1965).
(Frequency curves for wave heights in the Haringvliet).

[13] Opdam H.J.
Een mathematisch model van de kustzone, betreffende de invloed van golven, getij, wind en corioliskracht op de stroming langs de kust.
Rijkswaterstaat, Directie Waterhuishouding en Waterbeweging, Afdeling Kustonderzoek.
Studierapport W.W.K. 70-11.

[14] Frijlink, H.C.
Discussion des formules de débit solide de Kalinske, Einstein et Meyer-Peter et Mueller, compte tencée des vesures récentes de transport dans les rivières Neerlandaises.
2^{me} Journ. Hydraulique, Soc. Hydr. de France, Grenoble 1962, pp 98-103.

[15] Einstein, H.A.
The bed-load function for sediment transportation in open channel flow.
U.S. Dept. of Agr., Techn. Bull. nr. 1026, 1950.

[16] Vanoni, Vito A.
Transportation of suspended sediment by water.
Proc. ASCE, June 1944 (paper 2267, Trans. ASCE).

[17] Bakker, W.T.
The dynamics of a coast with a groyne system.
XI Conf. on Coastal Eng., London 1968.

[18] Bakker W.T., Klein Breteler E.H.J. and Roos A.
The dynamics of a coast with a groyne system.
XII Conf. on Coastal Eng., Washington D.C. 1970.

[19] Pelnard-Considère, R.
Essai de théorie de l'évolution des formes de rivages en plages de sable et de galet.
Quatrièmes Journées de l'Hydraulique, Paris, 13-15 Juin 1954.
Les Energie de la Mer, Question III.

[20] Bakker, W.T.
The relation between wave climate and coastal constants (unpublished yet).

[21] Longuet-Higgins, M.S.
Longshore currents, generated by obliquely incident sea waves.
J. of Geophysical Research, Vol. 75, no. 33, nov. 20, 1970.

[22] Mc Cowan, J.
On the highest wave of permanent type
Phil. Mag. (V) Vol. 38, pp 351-357.

[23] Munk, W.H.
The solitary wave theory and its application to surf problems.
Annals New York Academy of Sciences.

[24] Galvin, C.J.
Longshore current velocity: a review of theory and data.
Reviews of Geophysics, vol. 5, nr. 3, august 1967.

[25] Pierson, W.J. Jr.
Wind-generated gravity waves.
Advances in Geophysics, 2 : 93-178.
Academic Press, Inc. New York.

[26] Thornton, E.B.
Longshore current and sediment transport.
University of Florida, Gainesville, Florida, Dept. of Coastal and Oceanographic Engineering, Technical Report no. 5.

[27] Battjes, J.A.
Radiation stresses in short-crested waves.
J. of Mar. Res., vol. 30, nr. 1, 1972.

LIST OF ANNEXES

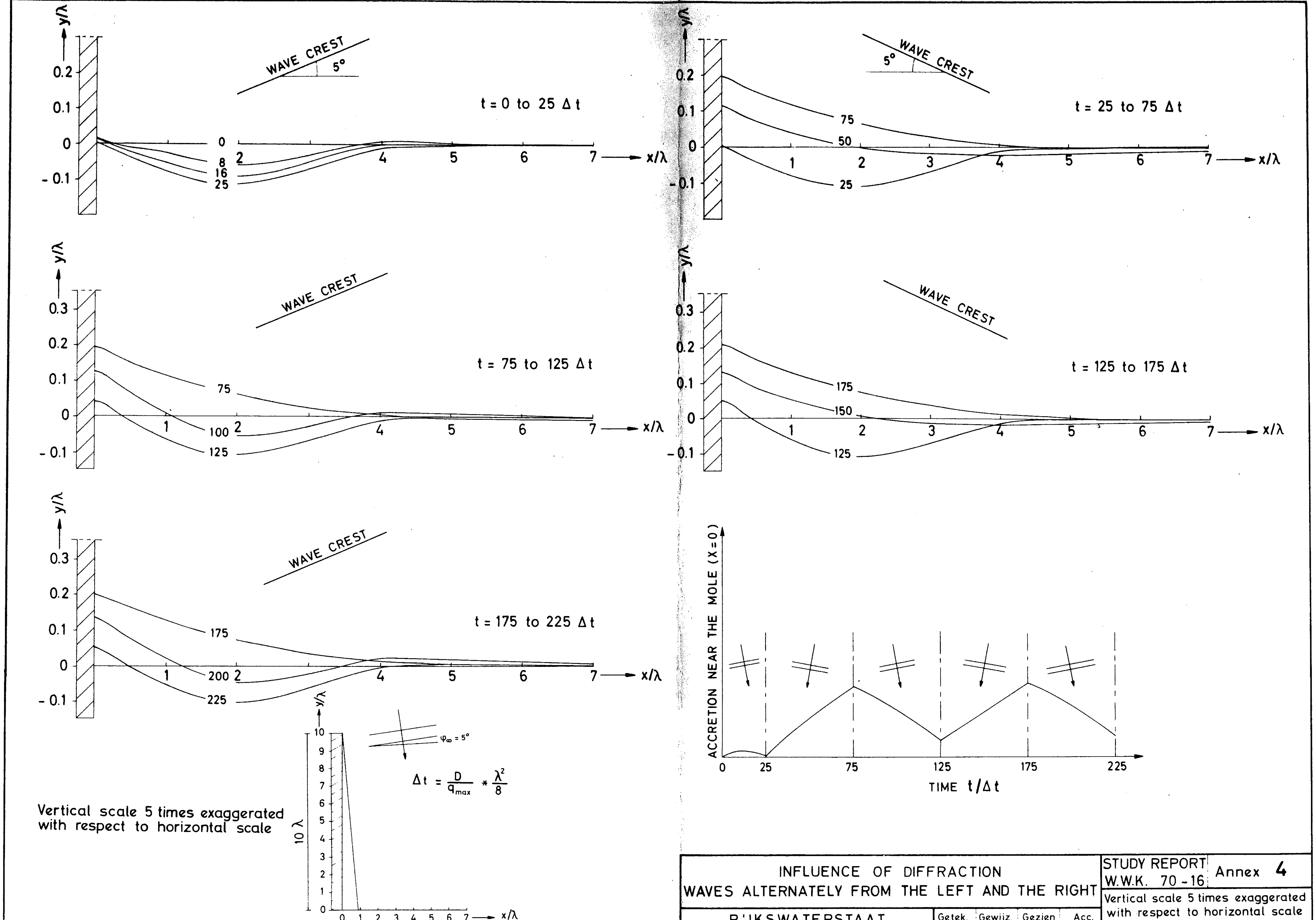

INFLUENCE OF DIFFRACTION
WAVES ALTERNATELY FROM THE LEFT AND THE RIGHT

STUDY REPORT W.W.K. 70 - 16 — Annex 4

Vertical scale 5 times exaggerated with respect to horizontal scale

RIJKSWATERSTAAT
DIRECTIE W. en W.
AFD. KUSTONDERZOEK

Getek.	Gewijz.	Gezien	Acc.

A2 Nr. 71.152

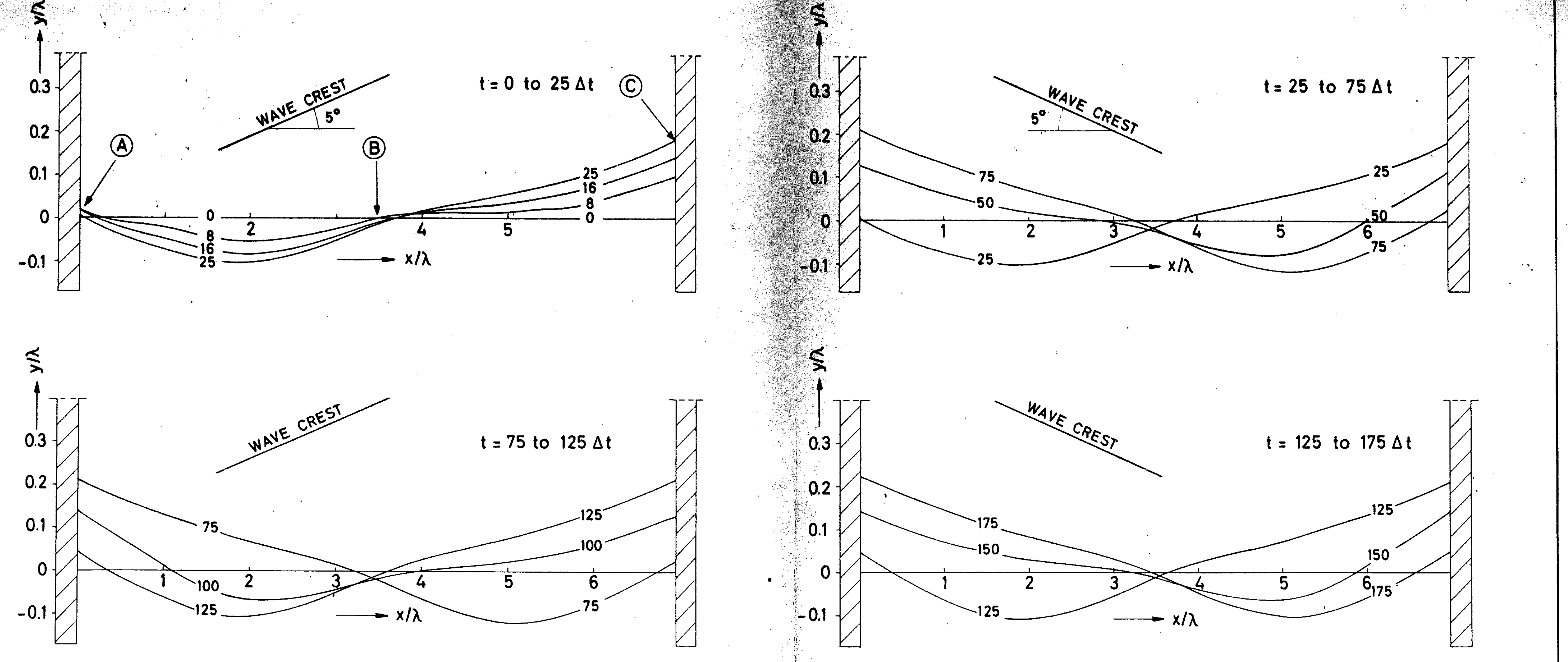

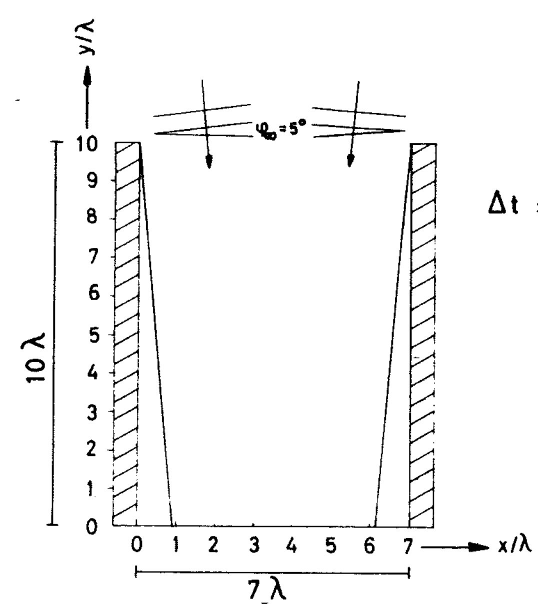

$$\Delta t = \frac{D}{q_{max}} * \frac{\lambda^2}{8}$$

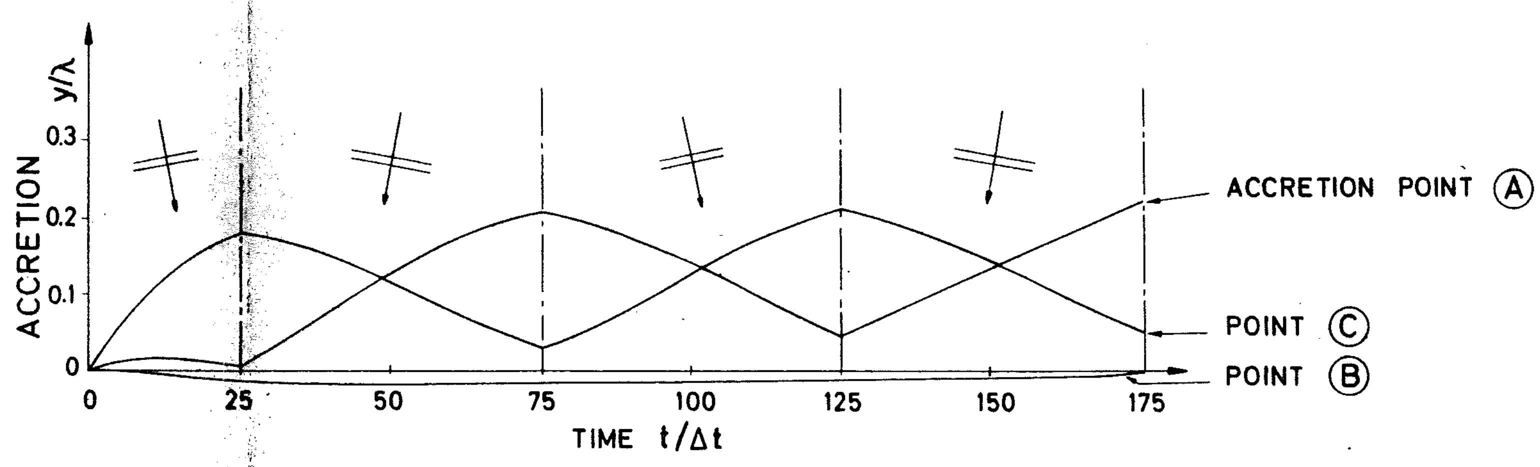

Vertical scale 5 times exaggerated with respect to horizontal scale

ONE - LINE THEORY COASTLINE BETWEEN TWO GROYNES WAVES ALTERNATELY FROM THE LEFT AND THE RIGHT					STUDY REPORT W.W.K. 70 - 16	Annex 5
RIJKSWATERSTAAT DIRECTIE W.en W. AFD. KUSTONDERZOEK	Getek.	Gewijz.	Gezien	Acc.	Vertical scale 5 times exaggerated with respect to horizontal scale	
					A 2	Nr 71.153